Published in final edited form as:
Life Sci. 2008 August 15; 83(7-8): 272–283. doi:10.1016/j.lfs.2008.06.020.

On the Mechanisms of Arrhythmias in the Myocardium of mXinα-Deficient Murine Left Atrial-Pulmonary Veins Tissue

Yu-Jun Lai, M.Sc.[*,H], **Eagle Yi-Kung Huang, Ph.D.**[**], **Hung-I Yeh, M.D., Ph.D.**[H], **Yen-Lin Chen, M.Sc.**[***], **Jim Jung-Ching Lin, Ph.D.**[I], and **Cheng-I Lin, Ph.D.**[***]

[*]Graduate Institute of Life Sciences, National Defense Medical Center, Taipei, Taiwan

[**]Institute of Pharmacology, National Defense Medical Center, Taipei, Taiwan

[***]Institute of Physiology, National Defense Medical Center, Taipei, Taiwan

[H]Department of Medical Research, Mackay Memorial Hospital and Mackay Medicine, Nursing and Management College, Taipei, Taiwan

[I]Department of Biological Sciences, University of Iowa, Iowa, USA

Abstract

We have previously shown that left atrial-pulmonary vein tissue (LA-PV) can generate reentrant arrhythmias (atrial fibrillation, AF) in wild-type (mXinα+/+) but not in mXinα-null (mXinα-/-) mice. With the present experiments, we investigated the arrhythmogenic activity and the underlying mechanisms in mXinα+/+ versus mXinα-/- LA-PV.

Electrical activity and conduction velocity (CV) were recorded in LA-PV by means of a MED64 system. CV was significantly faster in mXinα+/+ than in mXinα-/- LA-PV and it was increased by 1 μM isoproterenol (ISO). AF could be induced by fast pacing in the mXinα+/+ but not in mXinα-/- LA-PV where automatic rhythms could be present. ISO increased the incidence of AF in Xinα+/+ whereas it increased that of automatic rhythms in mXinα-/- LA-PV. In LA-PV with the right-atrium attached (RA-LA-PV), automatic rhythms occurred in all preparations. In mXinα+/+ RA-LV-PV simultaneously treated with ISO, strophanthidin and atropine, the incidence of the automatic rhythm was about the same, but AF increased significantly. In contrast, in mXinα-/- RA-LA-PV under the same condition, the automatic rhythm was markedly enhanced, but still no AF occurred. Conventional microelectrode techniques showed a longer APD_{90} and a less negative maximum diastolic potential (MDP) in mXinα-/- than mXinα+/+ LA-PV tissues. Whole-cell current clamp experiments also showed a less negative MDP in mXinα-/- versus mXinα+/+ LA-PV cardiomyocytes.

The fact that AF could be induced by fast pacing under several conditions in mXinα+/+ but not in mXinα-/- LA-PV preparations appears to be due to a slower CV, a prolonged APD_{90}, a less negative MDP and possibly larger areas of conduction block in mXinα-/- myocardial cells. In contrast, the non-impairment of automatic and triggered rhythms in mXinα-/- preparations may be due to the fact that the mechanisms underlying these rhythms do not involve cell to cell conduction.

Keywords

left atrial-pulmonary vein tissue; murine Xinα gene-KO; atrial fibrillation; triggered and automatic rhythms; fast pacing; cardioactive agents; multi-electrode mapping; conduction velocity; patch clamp

Correspondence to: Prof. Cheng-I Lin, Ph.D., Department of Physiology & Biophysics, National Defense Medical Center, 161, Sec 6, Min-Chuan East Road, Taipei 114, Taiwan, Fax: + 886 2 8792 4860, Tel: + 886 2 8792 4854, E-mail: bme03@ndmctsgh.edu.tw.

Introduction

Atrial fibrillation (AF) is the most common arrhythmia in the aged in all human societies. Clinical risk factors for the development of AF include age, gender, hypertension, diabetes mellitus, valvular heart diseases, heart failure, etc. The diversity of the risk factors renders the hope of a definitive control of AF unlikely (Oral, 2005; Gollob, 2006; Atienza and Jalife, 2007). Whether or not the susceptibility to the development of AF carries an underlying genetic background thus deserves attention, not only for a better clinical management, but also a possible better prevention (Pappone et al., 2006; Aksnes et al., 2007).

Many genes participate in the development and function of mammalian heart. Mutations in these genes lead to a wide variety of inherited human diseases (Saba et al., 2005; Temple et al., 2005; Gollob, 2006; Olson et al., 2006). In this connection, ectopic foci may initiate and maintain (Haissaguerre et al., 1998) paroxysmal AF as well as atrial tachycardia in the pulmonary veins tissue (PV) (Haissaguerre et al., 1998; Chen et al., 2000; Chen et al., 2001). The multilayered left atrial muscle (myocardial sleeve) spreading onto the proximal PV has a complex three-dimensional organization with disseminated myocardial clusters in the distal PV (Chen et al., 2000).

The occurrence of independent pulsations of PV is consistent with the demonstration that human PV contains P cells, transitional cells and Purkinje cells (Perez-Lugones et al., 2003). Therefore, abnormal automaticity has been suggested as a mechanism of PV arrhythmogenic activity (Haissaguerre et al., 1998). However, in our preliminary trials (Chen et al., 2007), focal tachyarrhythmias and AF were detected, which were induced by bursts of fast pacing in the absence and presence of cardioactive agents. Therefore, the mechanisms responsible for the arrhythmias originating from the PV could include enhanced automatic rhythms, triggered activity or AF (see Atienza and Jalife, 2007).

In this connection, we have shown that left atrial-pulmonary vein tissue (LA-PV) can generate AF in wild-type (mXinα+/+) but not in mXinα-deficient (mXinα-/-) mice (Song et al., 2005). This finding suggested the need to investigate the mechanism by which mXinα gene may play a role in the arrhythmias originating from the left atrial-pulmonary vein tissue.

The Xin gene was first cloned from the developing chicken heart (Wang et al., 1996; 1999). Xin gene contributes to regulate cardiac morphogenesis by participating in a BMP-Nkx2.5-MEF2C (bone morphogenetic protein-Nkx2.5-muscle enhancer factor 2C) pathway (Wang et al., 1999; Sinn, et al., 2002; Lin et al., 2005). The gene product has a region containing 16-amino acid repeats, called Xin repeats (Wang et al., 1999; Pacholsky et al., 2004; Lin et al., 2005; Cherepanova et al., 2006; Huang et al., 2006), and many conserved proline-rich regions. The Xin protein is specifically found in the myotendinous junctions of skeletal muscle and in the intercalated discs of cardiac muscle (Wang et al., 1999; Sinn et al., 2002; Lin et al., 2005).

In the mouse, there are two homologous genes, *mXinα* and *mXinβ*. mXinα co-localizes with N-cadherin and β-catenin at the intercalated discs and directly interacts with β-catenin (Lin et al., 2005; Choi et al., 2007). The chicken Xin co-immunoprecipitates with both β-catenin and N-cadherin obtained from embryonic heart lysates, suggesting that Xin is a part of the N-cadherin/β-catenin complex (Sinn et al., 2002). The Xin repeats in human homologue (hXinα, Cmya1) of Xinα have been shown to bind actin filaments in vitro (Pacholsky et al., 2004) and the hXinα also contains binding domains for filamin c and Mena/VASP, actin cytoskeleton regulators (Van der Ven et al., 2006). The hXinα has been mapped to 3p.21.1-21.3 chromosomal region by radiation hybrid analysis, a region which also contains a locus for

dilated cardiomyopathy with conduction defect-2 (Lin et al., 2005). Targeted deletion of *mXinα* in mice results in cardiac hypertrophy and cardiomyopathy with conduction defects (Gustafson-Wagner et al., 2007). These findings suggest that mXinα may also play a role in myopathic changes of cardiac function. An abnormal conduction could relevant to our finding that AF can occur in mXinα+/+ but not in mXinα-/- mice (Song et al., 2004), since abnormal conduction could disrupt the reentrant path.

The general aim of the present study was to investigate the role of mXinα deletion in the various types of arrhythmias (reentrant AF, triggered and automatic) (Atienza and Jalife, 2007) in the murine LA-PV and right atrial RA-LA-PV tissues. In particular, we explored whether mXinα deletion might affect differently automatic rhythms, triggered rhythms and AF.

The specific aims were to use both mXinα+/+ and mXinα-/- tissues to: (1) determine conduction velocity in the absence and presence of adrenergic agonist isoproterenol (ISO); (2) use both LA-PV and RA-LA-PV preparations, since the latter has a larger mass and includes RA pacemaker tissues; (3) apply fast pacing to test the induction of AF and triggered rhythms; (4) pace the preparations in the absence and presence of drugs that clinically may facilitate the onset of arrhythmias; and (5) analyze by means of a microelectrode technique and whole cell current clamp the action potential duration (APD), diastolic depolarization (phase 4 slope) and the maximum diastolic potential (MDP), since this information may be pertinent to account for the different forms of arrhythmias occurring in mXinα+/+ and mXinα-/- tissues.

Materials and Methods

All experimental protocols were approved according to the ROC Animal Protection Law (Scientific Application of Animals), 1998. The PCR genotyping of the mXinα+/+ or mXinα-/- animals was performed using tail DNA by the primer pairs described previously (Wang et al., 1999). Mice aged 4 to 6 months were used. As shown in our recent report (Gustafson-Wagner et al., 2007), fibrosis in mXinα-null murine myocardium is already observed at 3 months of age. We did not detect obvious electrophysiological abnormalities in mXinα-null mice prior to overt cardiomyopathy.

Isolation of left atrial-pulmonary vein (LA-PV) preparations

Mice were anesthetized with intraperitoneal injection of sodium pentobarbital (50 mg/kg). A mid-line thoracotomy was performed, the hearts excised, pulmonary veins and atria isolated and placed in 37 °C oxygenated Tyrode solution. The wet weights of LA-PV were about the same for mXinα+/+ and mXinα-/- mice (2.9±0.2 mg and 3.3±0.4 mg, respectively). Those of RA-LA-PV for mXinα+/+ and mXinα-/- mice were 7.0±0.5 mg and 6.0±0.5 mg, respectively. The differences between the weights of two groups of preparations were not significant ($P>0.05$). The Tyrode solution contained (in mM): NaCl 137, $NaHCO_3$ 15.5, NaH_2PO_4 0.7, $CaCl_2$ 1.8, KCl 4, $MgCl_2$ 1 and glucose 11.1. The solution was gassed with gas mixture (95% O_2, 5% CO_2, pH 7.2-7.4 at 37 °C). Before the experiments with MED64 Recording System, the MED probe (MED-P515A; Panasonic, Tokyo, Japan; each electrode: 50 × 50 μm, interpolar distance: 150 μm; Fig. 1) was soaked in 70% ethanol for 15 min and dried up. The surface of the probes was treated overnight at room temperature with 0.1% polyethylenimine and 25 mM borate buffer, pH 8.4. The probe surface was dried and rinsed three times with deionized water. Finally, the probes were immersed in Tyrode solution and put in an incubator until use.

Construction of activation map in tissue preparations

Murine LA-PV was placed over the multi-electrode array (Fig. 1A). Each side of this array was 1.45 mm in length. The right panel (Fig. 1B) shows the fast sweep-speed traces of the eight recording electrodes aligned vertically. The traces show a time-dependent shift in the peak

signals from the pacing point to the recording electrode, which was ≤ 1.45 mm away. Sweep-speed traces were differentiated into dV/dt traces, as illustrated in Fig. 1C. The distance between the minima of two differentiated signals was marked by green arrows, indicating the local activation time (LAT). The activation map (Fig. 1D) was then constructed by means of LAT between the two sites (Meiry et al., 2001).

Different types of rhythms

The types of rhythms were determined before and after 3 s of high-frequency pacing (3 ms pulse duration, applied at 10, 20 and 30 Hz consecutively, each frequency for 1 s, a procedure referred to hereafter as 10-30 Hz pacing or fast pacing). The rhythms were classified as automatic (spontaneously active), triggered (occurring immediately after termination of pacing) and reentrant rhythms (AF, with a frequency >18 Hz and duration >500 ms; Atienza and Jalife, 2007) as in our previous study (Song et al., 2005).

As it will be indicated, some experiments were conducted in the presence of isoproterenol (ISO), strophanthidin and atropine, singly or in combination. When all three drugs were present, they will be referred to as combined drugs.

Action potential recording in LA-PV tissues

The LA-PV preparation was pinned to the tissue bath, perfused with Tyrode solution and stimulated at 4 Hz with 2 ms pulses. The action potentials (APs) were recorded by means of glass microelectrodes filled with 3 M KCl and connected to an electrometer (WPI Duo 223, World Precision Instruments, New Haven, CT, USA). The action potential duration at 50 % and 90% repolarization levels (APD_{50} and APD_{90}, respectively), the maximum diastolic potential and diastolic depolarization were measured. Electrical events were displayed on an oscilloscope (model 4072, Gould Instruments, Cleveland, OH, USA) and simultaneously recorded by means of a model TA11 (Gould) recorder.

Isolation of LA-PV cardiomyocytes and whole cell patch-clamp

The murine hearts were perfused in a retrograde manner via a polyethylene tubing (0.35-mm outer diameter) inserted through the aorta and left ventricle into the left atrium. The free end of the polyethylene tubing was connected to a Langendorff perfusion column for perfusion with oxygenated Tyrode solution of the following composition (in mM): NaCl 137, KCl 5.4, $CaCl_2$ 1.8, $MgCl_2$ 0.5, HEPES 10 and glucose 11, at 37 °C. pH was adjusted to 7.4 with 1 N NaOH. The perfusate was replaced for 8 to 12 minutes with oxygenated Ca^{2+}-free Tyrode solution containing 300 units/mL collagenase (Sigma type I), 0.25 units/mL protease (Sigma, type XIV) and 1% albumin.

The LA-PVs were cut from the heart and placed in a dissection chamber containing Kraftbruehe (KB) solution of the following composition (in mM): KCl 85, $MgSO_4$ 5, KH_2PO_4 10, EGTA 10, taurine 20, glucose 20 and albumin 1%. pH was adjusted to 7.4 with 1 N KOH. The tissue was cut into fine pieces and gently shaken in 0.5 mL of KB solution until single cardiomyocytes were obtained. The solution was gradually changed to normal oxygenated Tyrode solution. The cells were allowed to equilibrate in the bath for at least 30 minutes before the experiments.

The whole-cell patch clamp was performed in cardiomyocytes by means of an Axopatch 1D amplifier (Axon Instruments, Union, CA, USA) at 35 °C as described previously (Loh et al., 1992; Chen et al., 2001; Chen et al., 2003). Borosilicate glass pipettes (1.8-mm OD) were used, with tip resistances of 3 to 5 MΩ. The pipette solution contained the following (in mM): KCl 20, K aspartate 110, $MgCl_2$ 1, Mg_2ATP 5, HEPES 10, EGTA 0.5, LiGTP 0.1, and Na_2 phosphocreatine 5, adjusted to pH 7.2 with 1 N KOH. Before formation of the membrane-pipette seal, tip potentials were zeroed in Tyrode solution. Junction potentials between the bath

and pipette solution (9 mV) were corrected for action potentials (APs) recording only. APs were measured during superfusion with normal Tyrode solution. The APs were recorded in current-clamp mode as described previously (Loh et al., 1992). A hyperpolarizing step from a holding potential of -50 mV to the testing potential of -55 mV was applied for 80 ms at the beginning of experiment. The area under the capacitive currents was divided by the applied voltage step to obtain the total cell capacitance. Voltage command pulses were generated with a 12-bit digital-to-analog converter controlled by pCLAMP software (Axon Instruments). Data were sampled at rates varying from 2 to 25 kHz. Recordings were low-pass filtered at half the sampling frequency.

Statistical analysis

The quantitative data are expressed as mean ± SEM. Data were compared between groups by Chi square test or Student's t test before and after drug treatments, $P < 0.05$ was considered statistically significant.

Results

Measurement of conduction velocity and conduction block in LA-PV tissues

The extracellular recording of electrical activity was carried out as illustrated in Figure 1 (see Methods). The conduction velocity (CV) between two recording sites was measured as illustrated in Figure 2 by dividing the distance between two sites by the LAT (Meiry et al., 2001). Measurements were carried out in Tyrode solution at 37 °C, but the effects of a low temperature (25 °C) and of tetrodotoxin (TTX) were also measured, as they would be expected to change the conduction velocity. Indeed, the time from the electrical stimulus to the wave peak was significantly longer at the lower temperature and more so with TTX treatment (Fig. 2A).

The average data are shown in the graph in Figure 2B. In $n = 5$, the conduction velocity in LA-PV preparations of wild-type mice was reduced significantly from 66±3 at 37 °C to 25±3 cm/s at 25 °C. Similarly, the conduction velocity was significantly reduced by TTX at 37 °C (32 ±9 cm/s) and more so at 25 °C (13±4 cm/s). These findings show that in the wild type LA-PV preparations conduction velocity is decreased by low temperature and TTX and these changes are detected by the MED64 system.

Activation maps, conduction velocity and conduction block in LA-PV tissues of wild-type and Xinα-deficient mice

Typical examples of activation maps of a wild-type and a mXinα-/- LA-PV tissue are shown in Figures 3A and B, respectively. The conduction velocity in mXinα-/- preparation was slower than that in the mXinα+/+ preparation (28 vs. 46 cm/s). The average data obtained in 10 mXinα+/+ and in 10 mXinα-/- preparations show that conduction velocity was significantly smaller in the mXinα-/- (29±3 cm/s) than in mXinα+/+ preparations (52±3 cm/s) (Fig. 3C). Also, there was a trend for the mXinα-/- preparations to have a larger area of conduction block (defined as the area with a conduction velocity ≤ 10 cm/s; Eijsbouts et al., 2004) (Fig. 3D).

Since the β-agonist ISO increases conduction velocity in the heart (Munger et al., 1994), it was tested also in these preparations. As shown in Figure 3C, ISO (1 μM) significantly increased the conduction velocity in mXinα+/+ from 52±3 to 85±8 cm/s, but barely changed that of mXinα-/- LA-PV (29±3 vs. 33±4 cm/s). In the presence of ISO, conduction block was not significantly different between mXinα+/+ and mXinα-/- LA-PV (Fig. 3D).

These results indicate a slower conduction velocity and a smaller increase in conduction velocity to adrenergic activation in the mXinα-/- compared to the mXinα+/+ preparations.

Different rhythms in mXinα+/+ and mXinα-/- LA-PV preparations without and with right atrium attached

The right-atrium was left attached to the LA-PV preparation (RA-LA-PV preparation, see boxed inset in Fig. 5), since some results might depend on the inclusion of right atrial pacemaker cells (Lu et al., 1965) and a larger mass of the preparations (Garrey, 1914;Wakimoto et al., 2001). In Figure 4, the tracings of electrical activities (8 sets aligned vertically and 8 sets aligned horizontally) from a RA-LA-PV preparation were recorded by means of the MED64 system. The origin of the electrical stimulation is indicated by a star located at the central bottom block. In each set of traces, the end of stimulation artifact (10-30 Hz for 3 s) was followed by the responses to fast pacing. In 10 of 64 recording sites, high frequency electrical activities with amplitude larger than 0.5 mV were observed.

In Figure 5, the induction of an episode of AF by 10-30 Hz pacing in the mXinα+/+ RA-LA-PV preparation is illustrated in greater detail. The preparation was rhythmically and regularly active (around 4 Hz) before pacing. Fast pacing-induced AF with a frequency of about 50 Hz and a duration of 9 s before the rhythms returned to the control value 12 s later. The sections of the trace in Figure 5A labeled with the letters **a**, **b** and **c** are shown at higher time base in Figure 5B. ISO and other cardioactive agents were also tested with regard to the onset of different rhythms, since they can clinically play a role. The electrical activity of a mXinα+/+ LA-PV is shown in Figure 6A in Tyrode solution and in Figure 6B in the presence of strophanthidin. Before and after 10-30 Hz pacing, the preparation was quiescent both in the absence or presence of strophanthidin. In the presence of both ISO (3 min) and strophanthidin, no spontaneous activity occurred, but fast pacing induced a 7 s triggered rhythm with a cycle length of about 400 ms. After 6 min exposure to ISO in the presence of strophanthidin, automatic activity was present with a cycle length of about 3 s. Fast pacing induced AF which had a frequency of 38 Hz and lasted for 3 s (Fig. 6D).

The importance of the presence of both ISO and strophanthidin is shown by the fact that when strophanthidin was removed from the solution (still in the presence of ISO at 24th min) pacing did not induced AF but only triggered activity which lasted for 1 s only (Fig. 6E).

The inclusion of pacemaker tissues of the right atrium (RA-LA-PV preparation) led to somewhat different effects of fast pacing. In a mXinα+/+ RA-LA-PV preparation, automatic activity (cycle length: 1250 ms) was present before pacing and overdrive suppression (disappearance of automatic activity for 12 s) was induced by fast pacing (Fig. 6F). The long overdrive suppression could have been due to pacing-induced release of acetylcholine by the vagus nerve endings in RA-LA-PV tissue (Lu et al., 1965). To test this possibility, atropine was added to the same preparation. Atropine shortened the basic cycle length from 1250 to 610 ms and inhibited overdrive suppression (after drive, the cycle length actually shortened to around 273 ms) (Fig. 6G).

Because ISO and strophanthidin fostered the induction of AF and triggered rhythms, and atropine abolished overdrive suppression, a combination of these drugs was given to find out whether fast pacing would induce AF and triggered rhythms in those preparations that did not develop any in the absence of the drugs.

As illustrated in Figure 7A, in control a mXinα+/+ RA-PV-LA preparation was spontaneously active with a cycle length of 480 ms. After fast pacing, the cycle length increased to 750 ms. In the presence of ISO, strophanthidin and atropine, the spontaneous rate became faster (cycle length 234 ms) and fast pacing induced an episode of AF (Fig. 7B). The traces recorded in Figure 7B are shown at faster time base on the right side of Figure 7, the same letters identifying the same trace segments. In the presence of cardioactive drugs, fast drive was followed by an irregular rhythm (panel a), which became AF within 9 s (panels *b* and *c*). AF had a frequency

of about 30 Hz and lasted for 3.2 s before the rhythm returned 12 s later to the value before pacing (cycle length around 330 ms) (panel d). The importance of RA for the genesis of AF was demonstrated by the fact that after removal of RA from the RA-LA-PV preparation, AF could no longer be induced (traces not shown).

In Figure 8, the electrical activity of a mXinα-deficient type (mXinα-/-) RA-PV-LA preparation was recorded in the absence (control) and in the presence cardioactive drugs (1 μM ISO, 10 μM stroph. and 0.1 μM atropine; panel B). In control, the fast drive led to an acceleration of discharge (compare the top right panel with the right **a** panel). In the presence of the combined drugs, the rate of discharge was higher and the fast drive modified the spontaneous rhythm little. Therefore, in mXinα-deficient type RA-PV-LA preparation fast drive did not lead to AF either in control or in the presence of combined drugs.

Average values of incidence of different rhythm in mXinα+/+ and mXinα-/- LA-PV and RA-LA-PV preparations in the absence and presence of drugs

The average results obtained with the different protocols are summarized in Table 1. In the mXinα+/+ LA-PV preparations AF and triggered rhythms occurred whereas in mXinα-/- LA-PV preparations automatic rhythms were more frequent (but not significantly) and triggered rhythm could occur, but no AF was present (Table 1).

In mXinα+/+ LA-PV preparations (no RA), in the presence of ISO (1 μM) the incidence of AF (4/10 vs. 2/10) and of triggered rhythms (6/10 vs. 4/10) was higher (but not statistically) as compared with drug-free tests. In mXinα-/- preparation (no RA), in the presence of ISO the incidence of automatic rhythms was higher than in mXinα+/+ LA-PV preparations (7/10 vs. 1/10) and that of triggered rhythms was the same (6/10 vs. 6/10). Still, no AF was observed in mXinα-/- preparations (Table 1).

Thus, adding ISO increased the incidence of triggered and AF in mXinα+/+ LA-PV and of automatic and triggered rhythms (but did not induce AF) in mXinα-/- LA-PV preparations. In all 10 mXinα+/+ and 10 mXinα-/- RA-LA-PV preparations (RA attached), automatic rhythms were present, the spontaneous cycle lengths being 455±90 vs. 623±75 ms, respectively (NS). AF occurred in 2/10 mXinα+/+ RA-LA-PV preparations, but again AF did not occur in mXinα-/- RA-LA-PV preparations (0/10). In mXinα+/+ RA-LA-PV preparations, in the presence of the combined drugs, the rate of the automatic rhythm was similar (cycle length 515±100 ms vs. drug-free control of 455±90 ms), but the incidence of AF increased significantly (5/10). The frequency and duration of AF in the mXinα+/+ RA-LA-PV preparations under the combined drug treatment were 41±23 Hz and 6.4±2.4 s, respectively.

In contrast, in mXinα-/- RA-LA-PV preparations, the combined drugs markedly increased the rate of the automatic rhythm (cycle length 206±18 ms vs. 623±75 ms in drug-free control, $P<0.05$)> Yet, no AF was induced by fast drive (0/10, $P<0.05$ with respect to mXinα+/+ preparations), as illustrated in Figure 8.

Thus, the presence of right atrium led to automatic discharge in all preparation and to the occurrence of AF in the mXinα+/+ RA-LA-PV preparations, but did modify the lack of induction of AF in mXinα-/- RA-LA-PV preparations. In the presence of the right atrium, the combined drugs increased the occurrence of pacing-induced AF in mXinα+/+ RA-LA-PV but there was no AF in mXinα-/- RA-LA-PV preparations, although in the latter the combined drugs enhanced automatic discharge. Therefore, in mXinα+/+ LA-PV preparations AF could be induced under basal conditions and its incidence was increased by ISO and by the combined drugs in the presence of the RA. In contrast, in mXinα-/- RA-LA-PV preparations AF was not induced under any of the conditions studied, including the presence of ISO, of the RA atrium or of combined drugs.

Cellular electrophysiology of mXinα+/+ and mXinα-/- cardiomyocytes

The AP configuration was studied in isolated LA-PV tissues driven electrically at 4 Hz. In Figure 9A, left panel, APD_{90} was 18 ms in a mXinα+/+ LA-PV cell (top trace) and 31 ms in a mXinα-/- LA-PV cell (bottom trace). In the right panel of Figure 9A, the superimposed AP traces show that the APD_{90} of the mXinα-/- was appreciably longer than that of the mXinα+/+ cell. As summarized in Table 2 and Figure 9D, results in 8 pairs of LA-PV tissues driven at 4 Hz revealed a significantly longer APD_{50} and APD_{90} in mXinα-/- vs. mXinα+/+ preparations.

Automatic activity was observed in the LA-PV cardiomyocytes isolated from both mXinα+/+ and mXinα-/- preparations. In Figure 9B, the last driven AP (indicated by the upward arrow) was followed by automatic APs in the cardiomyocytes of the mXinα+/+ (left panel) and of mXinα-/- (right panel) LV-PV preparations. For comparison, the AP traces of automatic cardiomyocytes isolated from mXinα+/+ and mXinα-/- LA-PV were superimposed in Figure 9C. As summarized in Fig. 9D and Table 2, the average MDP of 8 mXinα-/- cells (-65±3 mV) was lower (but not significantly) than that of the 2 mXinα+/+ cells (-68±2 mV).

In the remaining cardiomyocytes, no automatic rhythms were observed although electrical stimulation at 0.1 Hz could induce driven AP. In all cardiomyocytes (37 mXinα-/- cells, of which 29 driven and 8 automatic) the average MDP of mXinα-/- cells (-69±1 mV) was significantly less negative than the average MDP of 26 mXinα+/+ cardiomyocytes (-74±2 mV, $P<0.05$; 24 driven plus 2 automatic) (Fig. 9D and Table 2). The average diastolic slope of 37 mXinα-/- cardiomyocytes (18±4 mV/s) was not significantly different from those of 26 mXinα+/+ LA-PV cardiomyocytes (5±3 mV/s, $P>0.05$) (Table 2).

Discussion

Our findings show that the mXinα-/- LA-PV preparations had a slower conduction velocity which was increased but little by adrenergic activation with respect to the mXinα+/+ LA-PV preparations. Furthermore (although it did not reach statistical significance), the mXinα-/- LA-PV preparations had a larger area of conduction block. Also, ISO increased the incidence of triggered rhythms and AF in mXinα+/+ LA-PV and of automatic and triggered rhythms (but not of AF) in mXinα-/- LA-PV preparations. The presence of right atrium (right atrial pacemakers and larger tissue mass) led to automatic discharge in all preparations, but still no AF occurred in mXinα-/- RA-LA-PV. Cardioactive drugs increased the incidence of AF in mXinα+/+ RA-LA-PV but not in mXinα-/- RA-LA-PV preparations, although they enhanced the automatic discharge in the latter preparation. APD_{50} and APD_{90} were significantly longer and the MDP less negative in mXinα-/- preparations.

We conclude that mXinα deletion prevents the induction of AF, but does not impair automatic or triggered rhythms because it affects electrophysiological properties that are important for the induction of AF but not for automatic or triggered rhythms.

Non-critical role of tissue mass in the lack of AF inducibility in mXinα-/- preparations

According to critical mass theory (Garrey, 1914; Wakimoto et al., 2001), it should be difficult to induce AF in the heart of small animals (such as mice) due to a lack of a critical mass > 100-200 mm^2. Indeed, it is not easy to induce AF in the heart of small animals like the mouse (Garrey, 1914; Wakimoto et al., 2001; Nerbonne, 2004). However, focal AF could be induced by acetylcholine *in vivo* (Wakimoto et al., 2001) or by ISO in the murine LA-PV preparations (Song et al., 2005).

By means of extra-cellular recording with the MED64 system, the present experiments demonstrated the presence of focal AF in two tenths of mXinα+/+ in both LA-PV and RA-LA-PV preparations. That the tissue mass was not the critical factor in the lack of focal AF in

mXinα-/- LA-PV preparation is suggested by the fact that AF did not occur even when the tissue mass was increased by the attached right atrium. Furthermore, the combined drugs treatment increased significantly the incidence of AF in mXinα+/+ and yet the tissue mass was the same as in the absence of drugs.

Slow conduction velocity, conduction block and occurrence of AF in murine LA-PV

Conduction velocity and conduction block have close relationship with AF (Tamaddon et al., 2000; VanderBrink et al., 2000). Xin gene is co-localized with N-cadherin or Cx43 in myocardium of mouse (Sinn et al., 2002). In mXinα-/- mice, there is a significant decrease in the expression level of β-catenin, N-cadherin, and desmoplakin, which could be expected to compromise the integrity of the intercalated discs and functionally impair adhesion as well as gap junctions, leading to cardiac conduction defects (Gustafson-Wagner et al., 2007).

In support of such an expectation, the present experiments demonstrated a slower conduction velocity and larger areas of conduction block in mXinα-/- LA-PV preparations as compared to mXinα+/+ preparations. Slower conduction velocity in atrial preparation would be a risk factor for developing reentrant atrial tachyarrhythmias (Shiroshita-Takeshita et al., 2005; Weiss et al., 2005), but this may be a matter of degree. In Cx40-null mice, atrial but not ventricular conduction velocity is reduced by 30% and, consequently, atrial but not ventricular tachyarrhythmias are readily observed (Verheule et al., 1999). In contrast, in our experiments, the significantly slower conduction velocity in mXinα-/- LA-PV preparations was associated with a lack of AF induction compared with the appearance of focal AF in one third of mXinα +/+ LA-PV preparations. In this connection, it should be noted that the slower conduction velocity in mXinα-/- LA-PV preparations was associated with a greater percentage of areas of block. It is possible that the latter could have contributed to preventing the induction of the AF in the mXinα-/- LA-PV preparations by disrupting the paths for reentry. The diminished electronic interactions together with the longer action potentials might also hindered the incidence of AF. ISO significantly increased conduction velocity in Xinα+/+ preparation (Fig. 3C) and yet it increased the incidence of AF (Table 1), suggesting that the role of conduction velocity in the induction of AF can be modified by several factors, such as dispersion of repolarization or prolonged action potentials. Accordingly, experimentally different conditions may account for the fact that in KCNE1-null mouse heart an occasionally generated AF could be abolished by ISO (Temple et al., 2005).

That the areas of conduction block may disrupt the conditions for the induction of AF seems to be supported by the fact that islands of scar tissues abolish AF (Page et al., 2004). In this connection, the fibrosis that develops in the Xinα-null mice (Gustafson-Wagner et al., 2007) could be a contributing factor.

The effects of digitalis glycosides on cardiac arrhythmias are well documented (Gheorghiade et al., 2004; Vassalle and Lin, 2004). In our laboratory, we used strophanthidin to induce cardiac arrhythmias in the ventricular tissues of large animal (such as dog) (Lin and Vassalle, 1978) and failing human myocardium (Lee et al., 2004). Strophanthidin can induce calcium overload and triggered rhythms (Lin and Vassalle, 1978; Vassalle and Lin, 2004). While the combination of ISO and strophanthidin increased the incidence of AF in the mXinα+/+ LA-PV preparations (Fig. 6D and Table 1), it failed to do so in mXinα-/- preparation, again stressing the importance of normal cell-to-cell junctions in the genesis of AF.

In a previous publication (Lai et al., 2007), we reported that in the ventricles of Langendorff perfused hearts the incidence of pacing-induced ventricular tachycardia was significantly higher in isolated mXinα-null (vs. wild-type control, $P<0.05$). But the difference in ventricular reentrant arrhythmias (VF) between mXinα-/- and wild-type preparations was not significant (1/8 vs. 0/12, $P>0.05$). Also in ventricular myocytes, the transient inward current I_{ti} induced

on repolarization after a prolonged depolarization (3050 ms) was significantly larger in mXinα-/- than in wild-type ventricular myocytes. Thus the mXinα-/- preparations may be prone to the development of triggered (but not reentrant) arrhythmias.

Unpublished data from our laboratory show that there are differences in certain ionic currents between atrial and ventricular myocytes of the mXinα-null mice, possibly related to different ultrastructures (e.g. lack of T-tubules in atrial cells) (Ayettey and Navaratnam, 1978), excitation-contraction coupling and intracellular Ca^{2+} regulation (Forbes and van Niel, 1988; Berlin, 1995). The sodium current (I_{Na}) of mXinα-null atrial cardiomyocytes (in contrast to ventricular myocytes) was smaller than that of wild type mice. The threshold voltage for I_{Na} was around -60 mV and I_{Na} peaked between -40 to -30 mV (peak current 30% smaller in mXinα-/- atrial myocytes). The smaller I_{Na} in atrial myocytes could contribute to a different susceptibility to arrhythmias. However, we still need to learn more about the characteristics of I_{Na} and I_{ti} in atrial myocytes of the mXinα-null mice.

Xinα gene, automatic and triggered rhythms

mXinα gene deletion did prevent the induction of AF, but did not impair automatic or triggered rhythm or their enhancement by ISO or combined drugs (Table 1). These results appear to reflect the different mechanisms underlying different forms of activity.

The automatic rhythms were mostly related to RA pacemakers, since spontaneous rhythms were present in all the mXinα+/+ and mXinα-/- RA-LA-PV preparations studied. This suggests that mXinα gene deletion does not affect the pacemaking mechanism. This is also strongly supported by the fact that in the presence of ISO spontaneous discharge was present in all mXinα-/- LA-PV preparations. Also, the combined drugs treatment significantly shortened the spontaneous cycle length in mXinα-/- but not in mXinα+/+, in contrast to the fact that AF did not occur in mXinα-/- preparations (Table 1).

As for the triggered rhythms, the underlying mechanism is believed to be delayed afterdepolarizations which are induced by an electrogenic extrusion of calcium by the sodium-calcium exchange. The calcium extruded during diastole is released by a calcium overloaded sarcoplasmic reticulum (SR) (Vassalle and Lin, 2004). This mechanism readily accounts for the fact that triggered rhythms are induced by rapid pacing which increases the calcium loading.

Indeed, ISO could enhance triggered arrhythmias mostly by enhancing the calcium overloading of the cardiomyocytes (Vassalle and Lin, 2004; Yuan et al., 2007). Accordingly, ISO increased markedly the triggered rhythms in mXinα-/- LA-PV preparations.

Electrophysiological modifications

In the current-clamp mode of patch clamp experiments, automatic rhythms were observed in 8 of 37 cardiomyocytes isolated from mXinα-/- LA-PV, which had a less negative MDP than the mXinα+/+ LA-PV cardiomyocytes (Table 2, Fig. 9). The less negative MDP may influence the spontaneous discharge in mXinα-/- LA-PV preparations, but it was not associated with incidence of AF in these mXinα-/- LA-PV preparations. Still, it is likely that in the mXinα-/- LA-PV preparations the longer APD_{90} (Fig. 9A and D) may combine with the deficiency of cell-to-cell coupling and area of conduction block in preventing the induction of AF.

Conclusions

The present results show that automatic rhythms, triggered rhythms and induction of AF were affected differently by *mXinα* gene deletion. The results indicate that the induction of AF was consistently hindered in mXinα-deficient preparations even under conditions that enhance its induction mXinα+/+ preparations. The mechanisms that prevent the induction of AF in the

mXinα-/- preparations appear to involve a decrease in conduction velocity and longer action potentials (with a possible contribution of larger areas of conduction block): these changes apparently prevent the establishment of reentry paths. However, automatic and triggered rhythms were not suppressed in mXinα-/- preparations, since their underlying mechanisms do not depend on conduction, but rather on the pacemaker current (automatic rhythm) or calcium overload of the SR (triggered rhythms). Further *in vivo* experimentation is required to establish whether the present observations apply to intact animals, but the results illustrate how AF may critically depends on the absence of certain normal intercellular components.

Acknowledgments

The present works were supported by grants NSC94-2320-B016-035 and NSC95-2320-B016-013 (C.I.L.) from National Science Council, Taipei, research grant from Mackay Memorial Hospital (Y.J.L. and H.I.Y.), Taipei, Taiwan and grant R01 HL075015 from the NIH, USA (J.J.C.L.).

References

Aksnes TA, Flaa A, Strand A, Kjeldsen SE. Prevention of new-onset atrial fibrillation and its predictors with angiotensin II-receptor blockers in the treatment of hypertension and heart failure. Journal of Hypertension 2007;25(1):15–23. [PubMed: 17143167]

Atienza F, Jalife J. Reentry and atrial fibrillation. Heart Rhythm 2007;4(3 Suppl):S13–S16. [PubMed: 17336877]

Ayettey AS, Navaratnam V. The T-tubule system in the specialized and general myocardium of the rat. Journal of Anatomy 1978;127(1):125–140. [PubMed: 701190]

Berlin JR. Spatiotemporal changes of Ca^{2+} during electrically evoked contractions in atrial and ventricular cells. American Journal of Physiology - Heart & Circulatory Physiology 1995;269 (38):H1165–H1170.

Chen YL, Lai YJ, Chen YC, Huang EYK, Lin CI. Effect of heptanol on the conduction and arrhythmogenic activity in the left atrium-pulmonary veins of wild-type and Xinα-null mouse. (abstract). Journal of Electrocardiology 2007;40(4S):S6.

Chen YJ, Chen SA, Chang MS, Lin CI. Arrhythmogenic activity of cardiac muscle in pulmonary veins of the dog: implication for the genesis of atrial fibrillation. Cardiovascular Research 2000;48(2):265–273. [PubMed: 11054473]

Chen YJ, Chen SA, Chen YC, Yeh HI, Chan P, Chang MS, Lin CI. Effects of rapid atrial pacing on the arrhythmogenic activity of single cardiomyocytes from pulmonary veins: implication in initiation of atrial fibrillation. Circulation 2001;104(23):2849–2854. [PubMed: 11733406]

Chen YJ, Chen YC, Chen P, Lin CI, Chen SA. Temperature regulates the arrhythmogenic activity of pulmonary vein cardiomyocytes. Journal of Biomedical Science 2003;10(5):535–543. [PubMed: 12928594]

Cherepanova O, Oriova A, Galkin VE, van der Ven PFM, Furst DO, Jin JP, Egelman EH. Xin-repeats and nebulin-like repeats bind to F-actin in a similar manner. Journal of Molecular Biology 2006;356 (3):714–723. [PubMed: 16384582]

Choi S, Gustafson-Wagner EA, Wang Q, Harlan SM, Sinn HW, Lin JLC, Lin JJC. The intercalated disc protein, mXinα, is capable of interacting with β-catenin and bundling actin filaments. Journal of Biological Chemistry 2007;282(49):36024–36036. [PubMed: 17925400]

Eijsbouts SC, Houben RP, Blaauw Y, Schotten U, Allessie MA. Synergistic action of atrial dilation and sodium channel blockade on conduction in rabbit atria. Journal of Cardiovascular Electrophysiology 2004;15(12):1453–1461. [PubMed: 15610296]

Forbes MS, van Niel EE. Membrane systems of guinea pig myocardium: ultrastructure and morphometric studies. The Anatomical Record 1988;222(4):362–379. [PubMed: 2465704]

Garrey WE. The nature of fibrillary contraction of the heart: its relation to tissue mass and form. American Journal of Physiology 1914;33:397–414.

Gheorghiade M, Adams KF Jr, Colucci WS. Digoxin in the management of cardiovascular disorders. Circulation 2004;109(24):2959–2964. [PubMed: 15210613]

Gollob MH. Cardiac connexins as candidate genes for idiopathic atrial fibrillation. Current Opinion in Cardiology 2006;21(3):155–158. [PubMed: 16601450]

Gustafson-Wagner EA, Sinn HS, Chen YL, Wang DZ, Reiter RS, Lin JLC, Yang B, Williamson RA, Chen J, Lin CI, Lin JJC. Loss of mXinα, an intercalated disc protein, results in cardiac hypertrophy and cardiomyopathy with conduction defects. American Journal of Physiology - Heart & Circulatory Physiology 2007;293(5):H2680–H2692. [PubMed: 17766470]

Haissaguerre M, Jais P, Shah DC, Takahashi A, Hocini M, Quiniou G, Garrigue S, Le Mouroux A, Le Metayer P, Clementy J. Spontaneous initiation of atrial fibrillation by ectopic beats originating in the pulmonary veins. New England Journal of Medicine 1998;339(10):659–666. [PubMed: 9725923]

Huang HT, Brand OM, Mathew M, Ignatiou C, Ewen EP, McCalmon SA, Naya FJ. Myomaxin is a novel transcriptional target for MEF2A that encodes a Xin related α-actinin interacting protein. Journal of Biological Chemistry 2006;281(51):39370–39379. [PubMed: 17046827]

Lai YJ, Chen YY, Cheng CP, Lin JJC, Chudorodova SL, Roshchevskaya IM, Roshchevsky MP, Chen YC, Lin CI. Changes in ionic currents and reduced conduction velocity in hypertrophied ventricular myocardium of Xin alpha-deficient mice. Anatolian Journal of Cardiology 2007;7(Suppl 1):90–92. [PubMed: 17584692]

Lee FY, Wei J, Wang JJ, Liu HW, Shih TC, Lin CI. Electromechanical properties of Purkinje fiber strands isolated from human ventricular endocardium. Journal of Heart & Lung Transplantation 2004;23(6): 737–744. [PubMed: 15366435]

Lin CI, Vassalle M. Role of sodium in strophanthidin toxicity of Purkinje fibers. American Journal of Physiology 1978;234(4):H477–486. [PubMed: 645886]

Lin JJC, Gustafson-Wagner EA, Sinn HW, Choi S, Jaacks SM, Wang DZ, Evans S, Lin JLC. Structure, expression, and function of a novel intercalated disc protein, Xin. Journal of Medical Science 2005;25 (5):215–222.

Loh SH, Lee AR, Huang WH, Lin CI. Ionic mechanisms responsible for the antiarrhythmic action of dehydroevodiamine in guinea-pig isolated cardiomyocytes. British Journal of Pharmacology 1992;106(3):517–523. [PubMed: 1504737]

Lu HH, Lange G, Brooks CM. Factors controlling pacemaker action in cells of the sinoatrial node. Circulation Research 1965;17(5):460–471. [PubMed: 5843881]

Meiry G, Reisner Y, Feld Y, Goldberg S, Rosen M, Ziv N, Binah O. Evolution of action potential propagation and repolarization in cultured neonatal rat ventricular myocytes. Journal of Cardiovascular Electrophysiology 2001;12(11):1269–1277. [PubMed: 11761415]

Munger TM, Johnson SB, Packer DL. Voltage dependence of beta-adrenergic modulation of conduction in the canine Purkinje fiber. Circulation Research 1994;75(3):511–519. [PubMed: 8062424]

Nerbonne JM. Studying cardiac arrhythmias in the mouse--a reasonable model for probing mechanisms? Trends in Cardiovascular Medicine 2004;14(3):83–93. [PubMed: 15121155]

Olson TM, Alekseev AE, Liu XK, Park S, Zingman LV, Bienengraeber M, Sattiraju S, Ballew JD, Jahangir A, Terzic A. Kv1.5 channelopathy due to KCNA5 loss-of-function mutation causes human atrial fibrillation. Human Molecular Genetics 2006;15(14):2185–2191. [PubMed: 16772329]

Oral H. Mechanisms of atrial fibrillation: lessons from studies in patients. Progress in Cardiovascular Diseases 2005;48(1):29–40. [PubMed: 16194690]

Pacholsky D, Vakeel P, Himmel M, Lowe T, Stradal T, Rottner K, Furst DO, vander Ven PF. Xin repeats define a novel actin-binding motif. Journal of Cell Science 2004;117(Pt 22):5257–5268. [PubMed: 15454575]

Page, PL. Surgery for cardiac arrhythmias (Chapter 120). In: Zipes, DP.; Jalife, J., editors. Cardiac electrophysiology: from cell to bedside. Saunders; Pennsylvania: 2004. p. 1104-1115.

Pappone C, Augello G, Sala S, Gugliotta F, Vicedomini G, Gulletta S, Paglino G, Mazzone P, Sora N, Greiss I, Santagostino A, LiVolsi L, Pappone N, Radinovic A, Manguso F, Santinelli V. A randomized trial of circumferential pulmonary vein ablation versus antiarrhythmic drug therapy in paroxysmal atrial fibrillation: the APAF Study. Journal of the American College of Cardiology 2006;48(11):2340–2347. [PubMed: 17161267]

Perez-Lugones A, McMahon JT, Ratliff NB, Saliba WI, Schweikert RA, Marrouche NF, Saad EB, Navia JL, McCarthy PM, Tchou P, Gillinov AM, Natale A. Evidence of specialized conduction cells in

human pulmonary veins of patients with atrial fibrillation. Journal of Cardiovascular Electrophysiology 2003;14(8):803–809. [PubMed: 12890038]

Saba S, Janczewski AM, Baker LC, Shusterman V, Gursoy EC, Feldman AM, Salama G, McTiernan CF, London B. Atrial contractile dysfunction, fibrosis, and arrhythmias in a mouse model of cardiomyopathy secondary to cardiac-specific overexpression of tumor necrosis factor-α. American Journal of Physiology - Heart & Circulatory Physiology 2005;289(4):H1456–1467. [PubMed: 15923312]

Shiroshita-Takeshita A, Brundel BJ, Nattel S. Atrial fibrillation: basic mechanisms, remodeling and triggers. Journal of Interventional Cardiac Electrophysiology 2005;13(3):181–193. [PubMed: 16177845]

Sinn HW, Balsamo J, Lilien J, Lin JJC. Localization of the novel Xin protein to the adherens junction complex in cardiac and skeletal muscle during development. Developmental Dynamics 2002;225(1): 1–13. [PubMed: 12203715]

Song, CY.; Lai, YJ.; Loh, YX.; Chan, YC.; Lin, CI. Electrophysiological properties of the LA-PV tissue of X_{IN}-gene knockout mice. In: Hiraoka, M.; Ogawa, S.; Kodama, I.; Inoue, H.; Katoh, T., editors. Advances in Electrocardiology 2004, Proceedings of the 31st International Congress on Electrocardiology; Kyoto, Japan. June 26-July 1, 2004; 2005. p. 69-72.

Tamaddon HS, Vaidya D, Simon AM, Paul DL, Jalife J, Morley GE. High-resolution optical mapping of the right bundle branch in connexin40 knockout mice reveals slow conduction in the specialized conduction system. Circulation Research 2000;87(10):929–936. [PubMed: 11073890]

Temple J, Frias P, Rottman J, Yang T, Wu Y, Verheijck EE, Zhang W, Siprachanh C, Kanki H, Atkinson JB, King P, Anderson ME, Kupershmidt S, Roden DM. Atrial fibrillation in KCNE1-null mice. Circulation Research 2005;97(1):62–69. [PubMed: 15947250]

VanderBrink BA, Sellitto C, Saba S, Link MS, Zhu W, Homoud MK, Estes NA 3rd, Paul DL, Wang PJ. Connexin40-deficient mice exhibit atrioventricular nodal and infra-Hisian conduction abnormalities. Journal of Cardiovascular Electrophysiology 2000;11(11):1270–1276. [PubMed: 11083248]

Van der Ven PFM, Ehler E, Vakeel P, Eulitz S, Schenk JA, Milting H, Micheel B, Furst DO. Unusual splicing events result in distinct Xin isoforms that associate differentially with filamin c and Mens/ VASP. Experimental Cell Research 2006;312(11):2154–2167. [PubMed: 16631741]

Vassalle M, Lin CI. Calcium overload and cardiac function. Journal of Biomedical Science 2004;11(5): 542–565. [PubMed: 15316129]

Verheule S, van Batenburg CA, Coenjaerts FE, Kirchhoff S, Willecke K, Jongsma HJ. Cardiac conduction abnormalities in mice lacking the gap junction protein connexin40. Journal of Cardiovascular Electrophysiology 1999;10(10):1380–1389. [PubMed: 10515563]

Wakimoto H, Maguire CT, Kovoor P, Hammer PE, Gehrmann J, Triedman JK, Berul CI. Induction of atrial tachycardia and fibrillation in the mouse heart. Cardiovascular Research 2001;50(3):463–473. [PubMed: 11376622]

Wang DZ, Hu X, Lin JLC, Kitten GT, Solursh M, Lin JJC. Differential displaying of mRNAs from the atrioventricular region of developing chicken hearts at stages 15 and 21. Frontier in Biosciences 1996;1:a1–a15.

Wang DZ, Reiter RS, Lin JLC, Wang Q, Williams HS, Krob SL, Schultheiss TM, Evans S, Lin JJC. Requirement of a novel gene, Xin, in cardiac morphogenesis. Development 1999;126(6):1281–1294. [PubMed: 10021346]

Weiss JN, Qu Z, Chen PS, Lin SF, Karagueuzian HS, Hayashi H, Garfinkel A, Karma A. The dynamics of cardiac fibrillation. Circulation 2005;112(8):1232–1240. [PubMed: 16116073]

Yuan Q, Fan GC, Dong M, Altschafl B, Diwan A, Ren X, Hahn HH, Zhao W, Waggoner JR, Jones LR, Jones WK, Bers DM, Dorn GW 2nd, Wang HS, Valdivia HH, Chu G, Kranias EG. Sarcoplasmic reticulum calcium overloading in junctin deficiency enhances cardiac contractility but increases ventricular automaticity. Circulation 2007;115(3):300–309. [PubMed: 17224479]

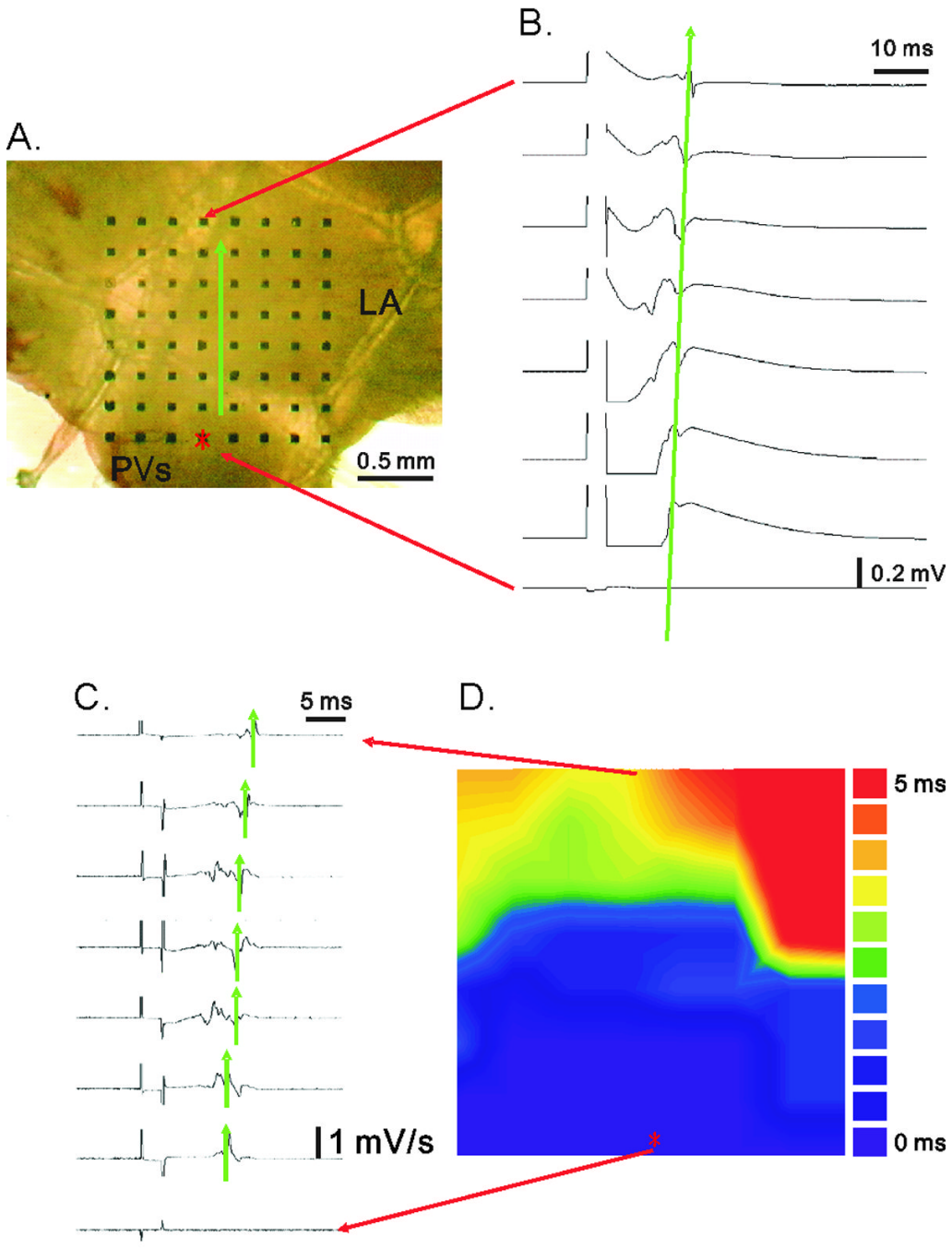

Figure 1.

Panel A illustrates the placement of murine LA-PV tissue over the multi-electrode array. Panel B illustrates sweep-speed traces of electrical potentials recorded extracellularly between two of 64 sites. The traces in millivolts were differentiated into dV/dt traces in panel C. The constructed activation map is shown in panel D. LA: left atrium; PV: pulmonary vein.

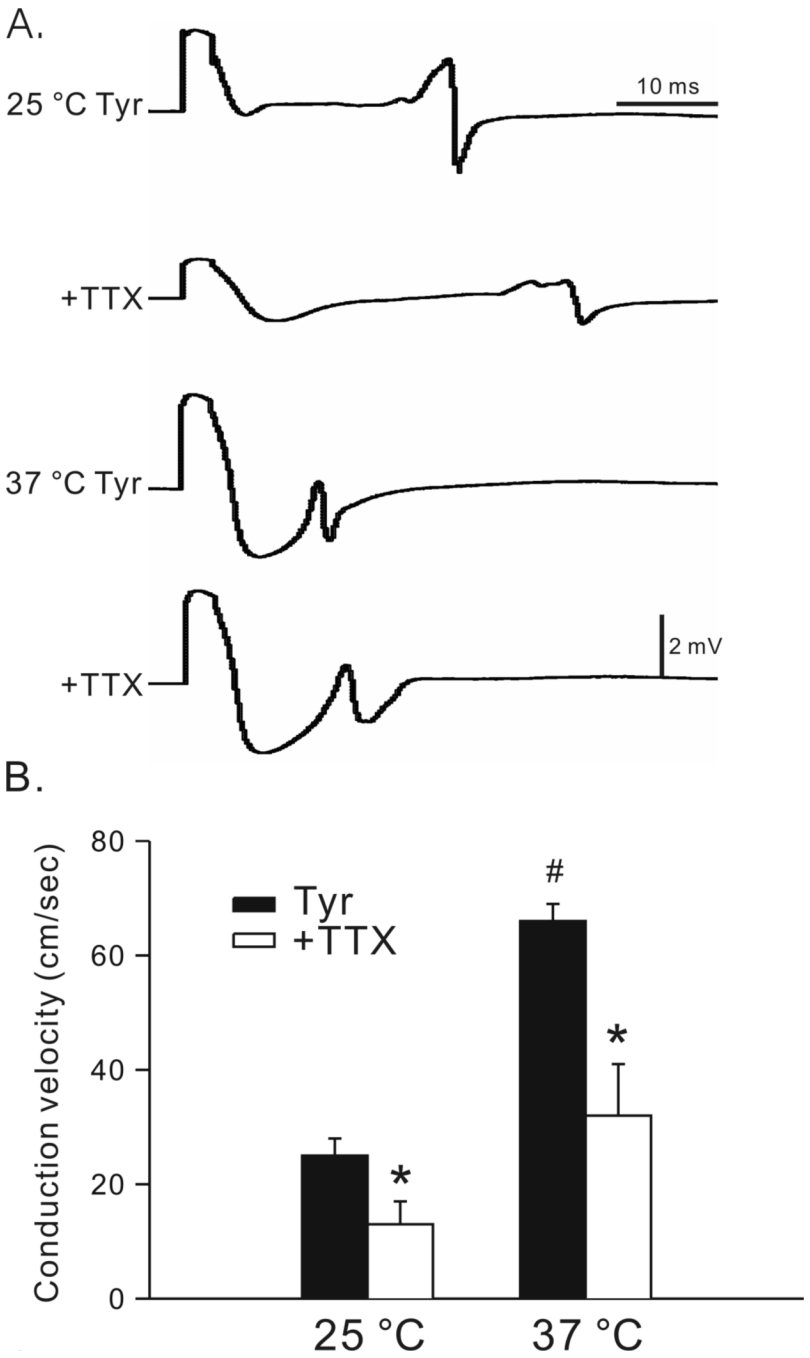

Figure 2.

Effects of low temperature and tetrodotoxin on conduction velocity. Panel A shows the effects of reducing temperature in Tyrode solution (25 °C Tyr and 37 °C Tyr) and in the presence of 3 μM tetrodotoxin (TTX, 25 °C +TTX and 37 °C +TTX) on conduction velocity of LA-PV preparations. Results of 5 experiments are summarized in panel B. The ordinate indicates the conduction velocity in centimeters per second at 25 °C vs. 37 °C before and after TTX treatment. $^{\#}$, $P < 0.05$, between 25 vs. 37 °C; *, $P < 0.05$, before and after treatment with TTX.

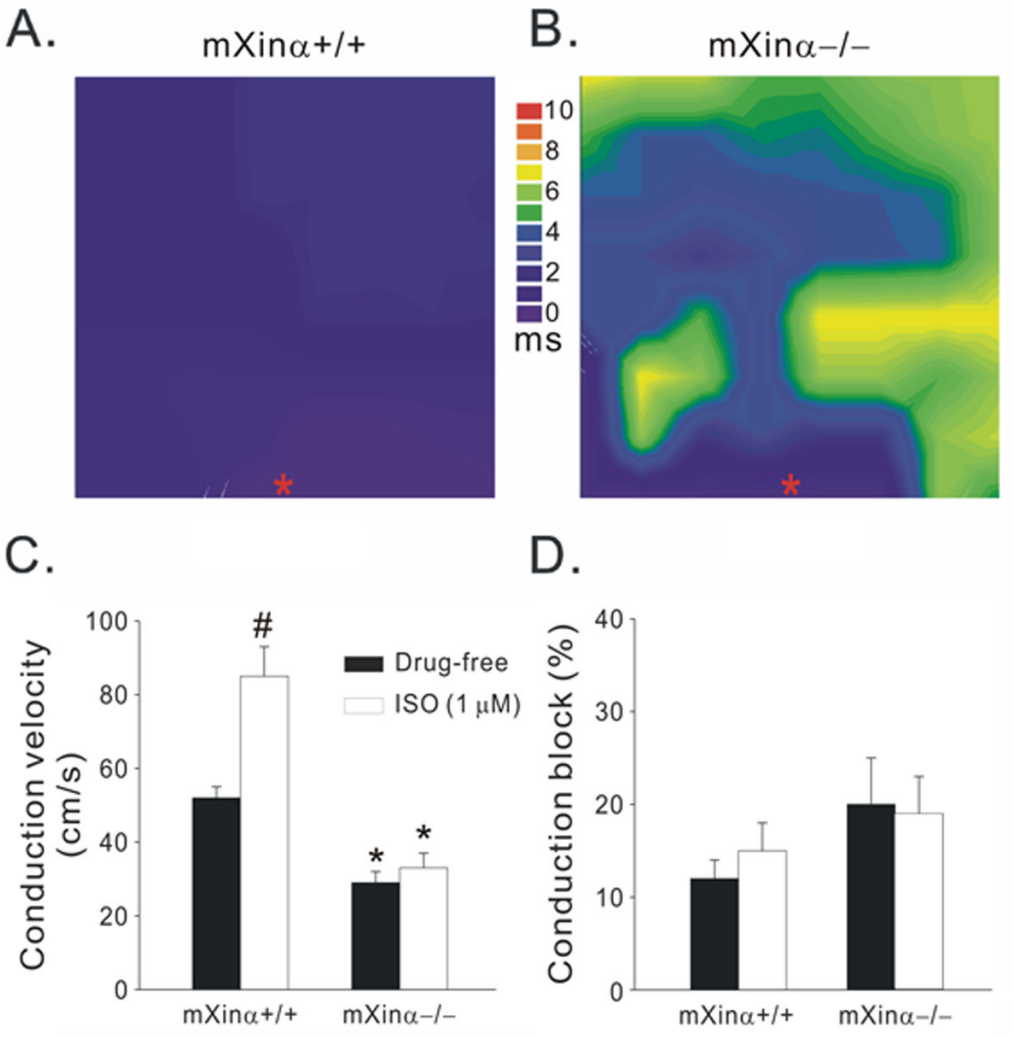

Figure 3.

Activation maps of wild-type (mXinα+/+, A) and Xinα-deficient (mXinα-/-, B) LA-PV tissue, showing conduction velocity (C) and conduction block (D) in the absence and presence of 1 μM isoproterenol (ISO). The conduction block was defined as an apparent local conduction velocity slower than 10 cm/s. n = 10; #, $P < 0.05$, drug-free vs. ISO; *, $P < 0.05$, Xinα+/+ vs. Xinα-/-.

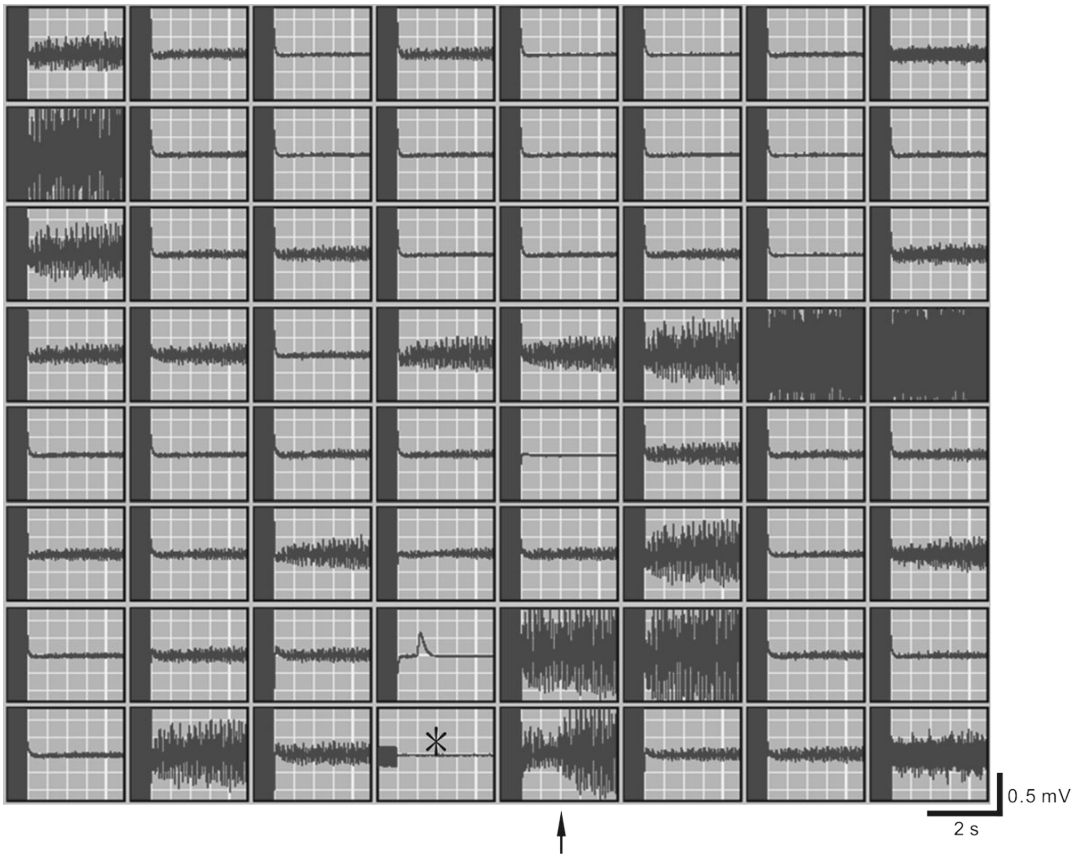

Figure 4.

Extracellular recordings of electrical activities in a RA-LA-PV preparation with a MED64 system. The 64 traces were aligned vertically and horizontally. Origin of electrical stimulation is indicated by the star located in the central bottom block. In each set of traces, the end of stimulation artifacts (10-30 Hz for 3 s) was followed by responses to the fast pacing. The trace (indicated by an arrow) to the right of the site of electrical stimulation was magnified and shown in Figure 5.

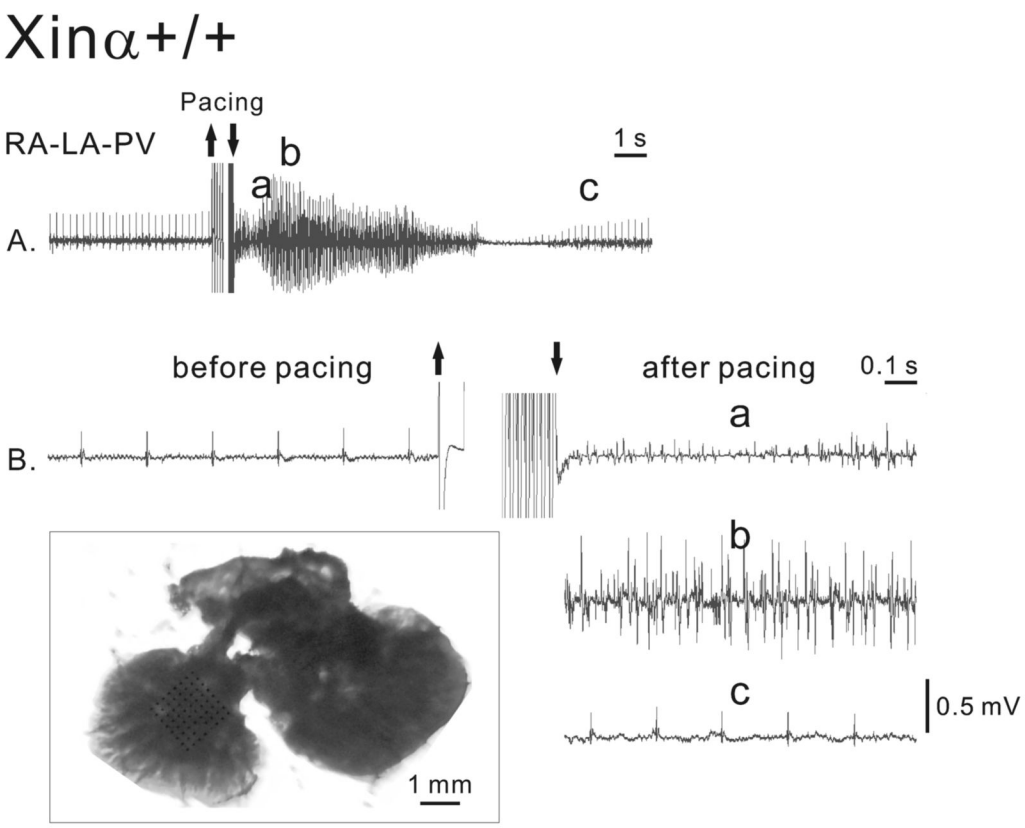

Figure 5.

Electrical activity of a wild-type (mXinα+/+) recorded with the MED64 system in a RA-LA-PV preparation perfused in Tyrode solution. The top panel shows the extracellular recordings at a slow speed. The lower panels show the fast-speed recordings before and after the 10-30 Hz pacing for 3 s in Tyrode solution. The sections of the trace after pacing labeled with **a, b** and **c** in panel A are identified by the same letters in panel B. The boxed inset shows a picture of a RA-LA-PV preparation with the multi-electrode array placed over LA. Bar = 1 mm. RA: right atrium; LA: left atrium; PV: pulmonary vein.

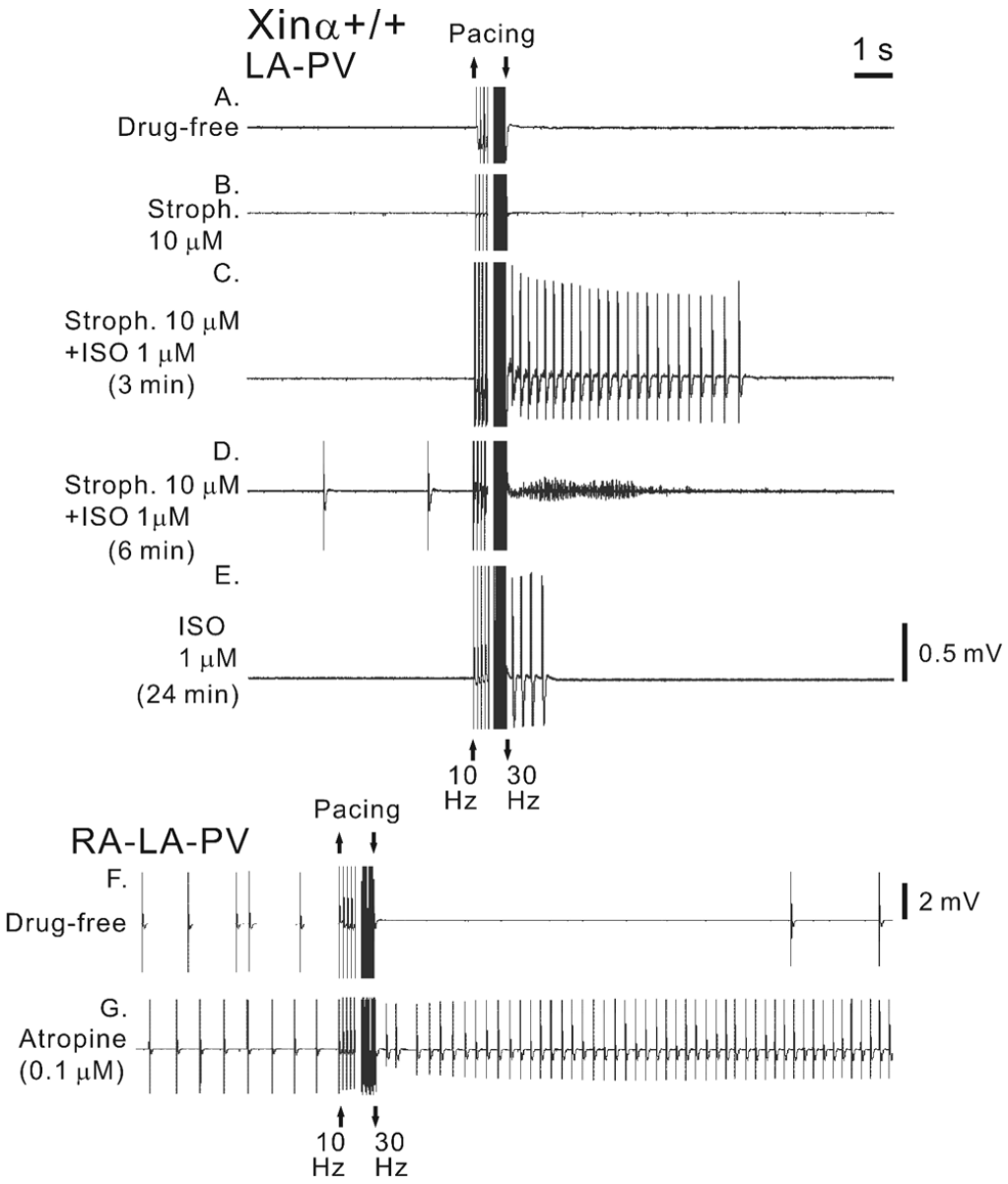

Figure 6.

Automatic activity and AF in a wild-type (mXinα+/+) LA-PV preparation in the absence and presence of cardioactive agents recorded with the MED64 system. Fast pacing (10-30 Hz for 3 s) was applied in the absence of drug treatment (drug free, panel A), during exposure to strophanthidin for 12 min (stroph., 10 μM; panel B), during exposure to strophanthidin and isoproterenol for 3 min (ISO, 1 μM) (panel C) and for 6 min (panel D), and during exposure to ISO only (panel E). A mXinα+/+ RA-LA-PV preparation was paced in the absence of drugs (panel F) and in the presence of atropine (0.1 μM) (panel G).

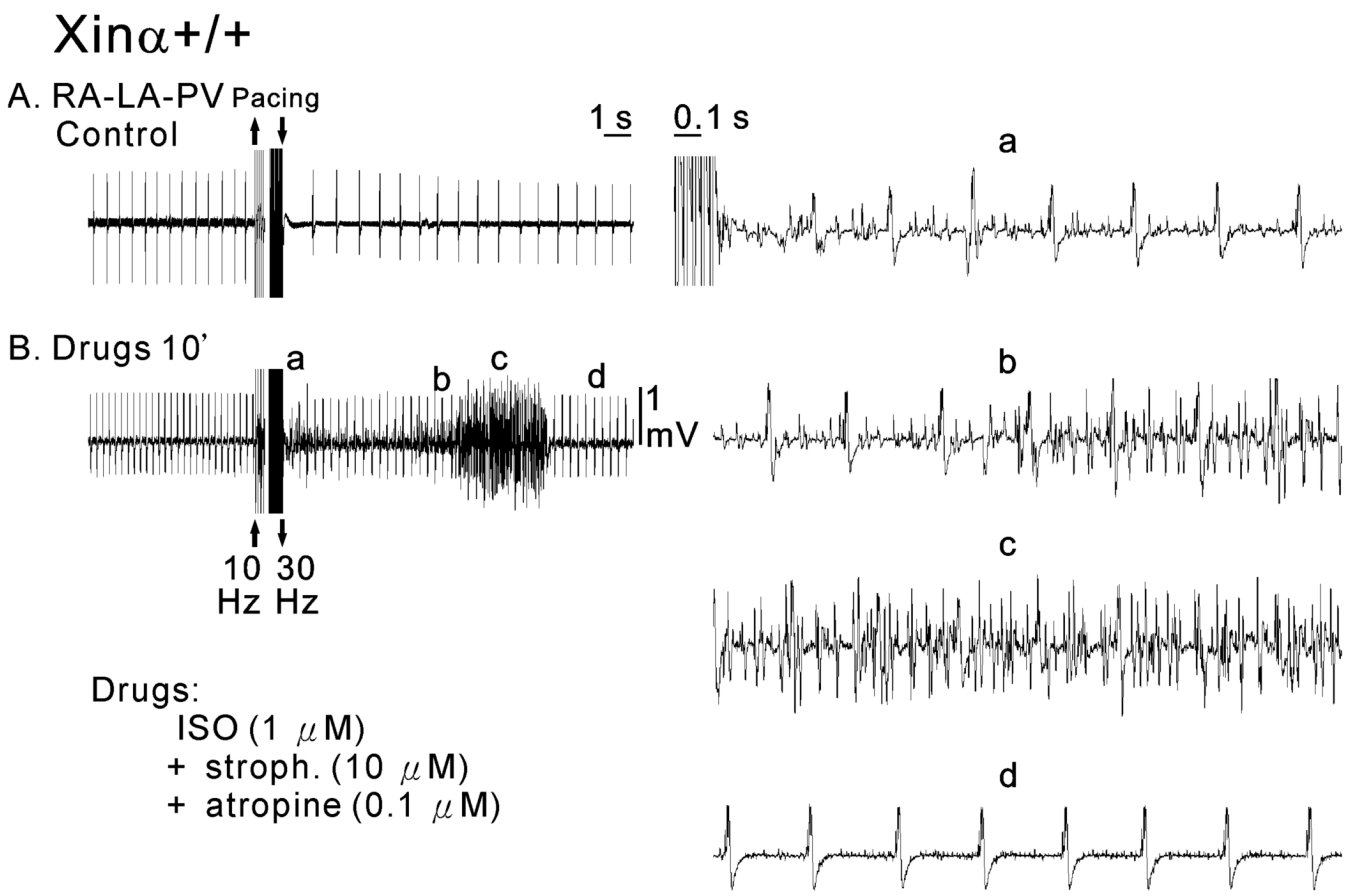

Figure 7.

Electrical activity of a wild-type (mXinα+/+) RA-PV-LA preparation in the absence (panel A) and presence (panel B) of cardioactive drugs (1 μM ISO, 10 μM stroph. and 0.1 μM atropine) recorded with the MED64 system. The right panels show the fast-speed recordings after pacing in the presence of cardioactive drugs at three time points (indicated by **a, b** and **c**).

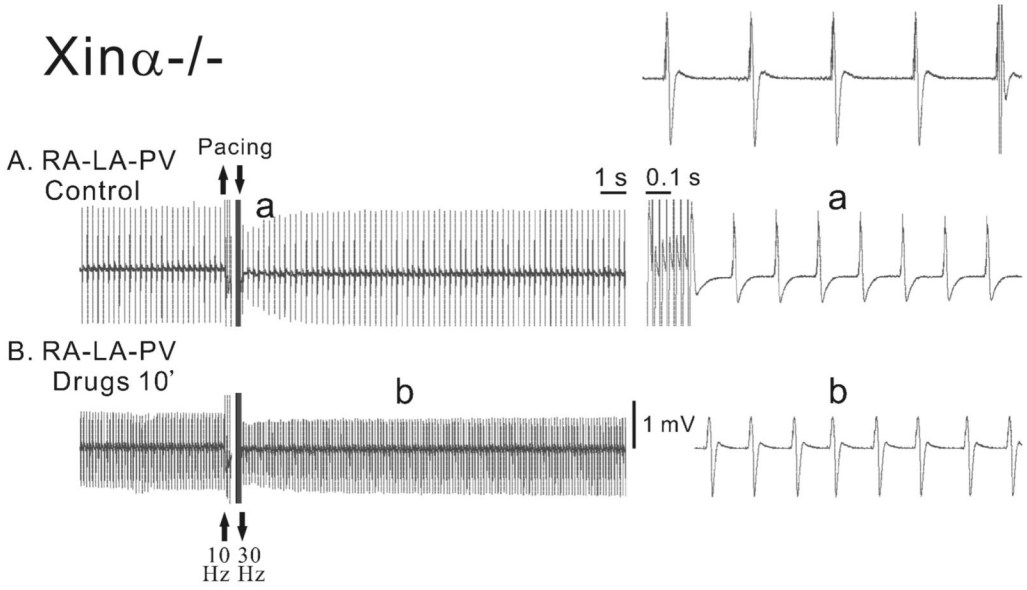

Figure 8.

Electrical activity of a mXinα-deficient type (mXinα-/-) RA-PV-LA preparation recorded with the MED64 system in the absence (panel A) and presence of cardioactive drugs (1 μM ISO, 10 μM stroph. and 0.1 μM atropine; panel B). The top right panel shows the fast-speed recordings before pacing in control solution. Combined drugs were added between panels A and B. The right panels show fast-speed recordings in the absence (panel **a**) and the presence (panel 5**b**) of the combined drugs at two time points indicated by the letters.

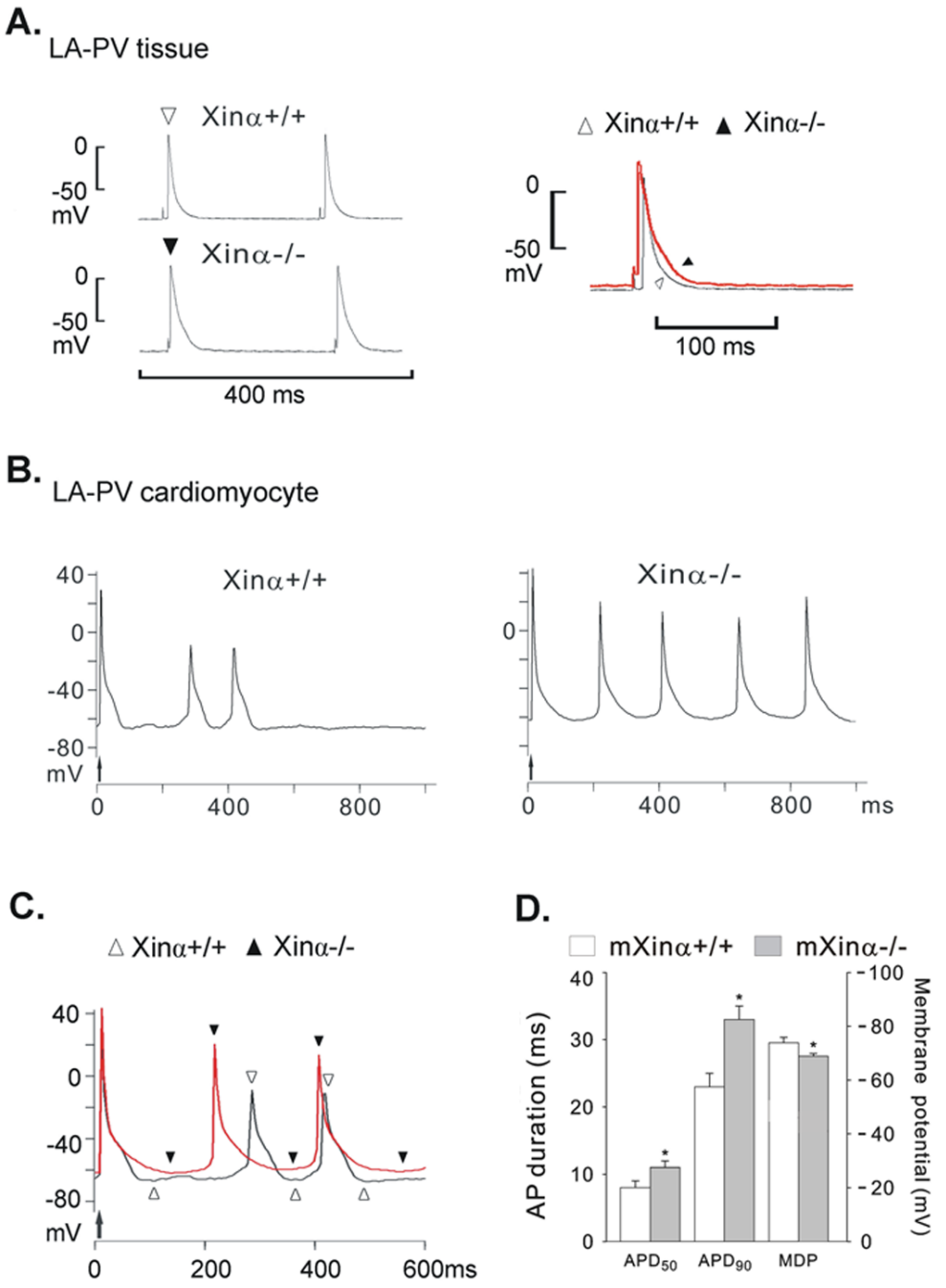

Figure 9.

Action potentials recorded from LA-PV preparations of a wild-type (mXinα+/+) and a mXinα-deficient (mXinα-/-) mice. In panel A, the action potentials (APs) from the mXinα+/+ (open triangle) and the mXinα-/- (solid triangle) preparation were superimposed. In panel B, the driven AP is indicated by an upward arrow and was followed by automatic APs. In panel C, traces of automatic APs of mXinα+/+ (open triangles) and mXinα-/- (solid triangles) cardiomyocytes were superimposed. In panel D, the graph shows the average values of action potential duration (APD_{50} and APD_{90}) in 8 mXinα+/+ and 8 mXinα-/- LA-PV preparations. The differences in maximum diastolic potential (MDP) of 26 mXinα+/+ and 37 mXinα-/- LA-

PV preparations are statistically significant. *, $P<0.05$ by Student's t test between mXinα+/+ and mXinα-/- LA-PV preparations.

Table 1

Effects of isoproterenol (ISO) and other cardio-active agents on rhythms of LA-PV or RA- LA-PV tissues of wild-type and mXin-deficient mice.

[] Rhythms		Automatic rhythms	Triggered rhythms	Atrial fibrillation
† LA-PV (Drug-free)	mXinα+/+	1/10	4/10	2/10
	mXinα-/-	3/10 (‡ SCL: 307±77 ms)	2/10	0/10
† LA-PV (ISO 1 μM)	mXinα+/+	1/10 (‡ SCL: 200 ms)	6/10	4/10
	mXinα-/-	7/10* (‡ SCL: 327±31 ms)	6/10	0/10*
†† RA-LA-PV (Drug-free)	mXinα+/+	(‡ SCL :455±90 ms) 10/10		2/10
	mXinα-/-	(‡ SCL :623±75 ms) 10/10		0/10
†† RA-LA-PV (Combined drugs)	mXinα+/+	(‡ SCL:515±100 ms) 10/10		5/10
	mXinα-/-	(‡ SCL:206±18 ms #) 10/10		0/10*

[] Three types of rhythms (automatic, triggered and atrial fibrillation) (Atienza and Jalife, 2007) observed in LA-PV or right atrial (RA)-LA-PV tissues of wild-type (mXinα+/+) and mXin-null (mXin α-/-) mice.

† LA-PV preparations were driven at 3 Hz in control Tyrode solution (Drug-free) or in Tyrode solution containing 1 μM isoproterenol (ISO 1 μM).

†† RA-LA-PV preparations were perfused either in drug-free solution or in Tyrode solution containing combined drugs (1 μM ISO plus 10 μM strophanthidin and 0.1 μM atropine) and then subjected to high-frequency supra-threshold electrical stimulation at 10-30 Hz for 3 sec.

‡ SCL, steady-state spontaneous cycle length.

# $P<0.05$, significant difference in the values of SCL in the presence of combined drugs as compared to values in drug-free solution by paired Student's *t* test.

* $P<0.05$, significant difference in the incidence of reentrant rhythms or automatic rhythms between mXinα+/+ and mXin α-/- by χ^2 analysis.

Table 2

Electrophysiological characteristics of LA-PV tissues and spontaneously active LA-PV cardiomyocytes obtained from wild-type and Xinα-deficient mice.

# Genotype	n	Xinα+/+	n	Xinα-/-
LA-PV tissues				
† Incidence of autom. tissues		2/10		6/14
†† Spont. cycle length, ms	2	1851±1106	6	537±189
‡ MDP, -mV	10	79±2	14	68±4*
‡ APA, mV	8	91±3	8	88±4
‡ APD_{50}, ms	8	8±1	8	11±1*
‡ APD_{90}, ms	8	23±2	8	33±2*
Cardiomyocytes				
Incidence of autom. cells		2/26		8/37
§ APA, mV	26	87±4	37	95±3
§ APD_{50}, ms	26	15±1	37	13±1
§ APD_{90}, ms	26	58±4	37	54±3
Spont. cycle length, ms	2	568±296	8	470±102
§ MDP, -mV	26	74±2	37	69±1*
§ Phase-4 slope, mV/s	26	5±3	37	18±4
[] MDP of autom. Cells, -mV	2	68±2	8	65±3
[] Phase-4 slope of autom. cells, mV/s	2	28±19	8	43±6

Genotypes of LA-PV preparations: mXin α+/+, wild-type mice; mXinα-/-, Xinα-deficient mice; LA-PV tissues vs. cardiomyocytes.

† Incidence of automatic (autom.) preparations, numbers of cells showing spontaneous activity over total numbers of cardiac preparations measured in each group.

†† Spontaneous (Spont.) cycle length indicates cycle length in ms of spontaneous AP; n, number of preparation.

‡ Action potential (AP) parameters of LA-PV tissues driven at 4 Hz. MDP, maximum diastolic potential; APA, AP amplitude; APD_{50} and APD_{90}, AP duration at 50% and 90% repolarization level, respectively.

§ Action potential parameters of 26 mXin α+/+ and 37 mXinα-/- LA-PV cardiomyocytes at 0.1 Hz basic electrical stimulation. Abbreviations MDP, APA and APD are similar to those of tissues. Of these cardiomyocytes, 2 mXin α+/+ and 8 mXinα-/- cells showed spontaneous APs.

[] The automatic APs were recorded immediately after the last driven beat (at 0.1 Hz electrical stimulation). Phase-4 slope, slope of diastolic depolarization in mV/s.

* Significantly different from mXinα+/+ myocytes (P<0.05).